



OPEN ACCESS

EDITED BY
Abdul Raheem,
Sukkur IBA University, Pakistan

REVIEWED BY
Vinay Kumar Tyagi,
National Institute of Hydrology
(Roorkee), India
Shakil Ahmed Jiskani,
Sukkur IBA University, Pakistan
Riaz Ahmad,
Yibin University, China

*CORRESPONDENCE
Khalideh Al Bkoo Alrawashdeh,
khalideh19@bau.edu.jo

SPECIALTY SECTION
This article was submitted to Sustainable
Process Engineering,
a section of the journal
Frontiers in Chemical Engineering

RECEIVED 21 June 2022
ACCEPTED 18 July 2022
PUBLISHED 26 August 2022

CITATION
Al Bkoo Alrawashdeh K, Al-Zboon KK,
Rabadi SA, Gul E, AL-Samrraie LA, Ali R
and Al-Tabbal JA (2022), Impact of Iron
oxide nanoparticles on sustainable
production of biogas through anaerobic
co-digestion of chicken waste
and wastewater.
Front. Chem. Eng. 4:974546.
doi: 10.3389/fceng.2022.974546

COPYRIGHT
© 2022 Al Bkoo Alrawashdeh, Al-
Zboon, Rabadi, Gul, AL-Samrraie, Ali and
Al-Tabbal. This is an open-access article
distributed under the terms of the
[Creative Commons Attribution License
\(CC BY\)](https://creativecommons.org/licenses/by/4.0/). The use, distribution or
reproduction in other forums is
permitted, provided the original
author(s) and the copyright owner(s) are
credited and that the original
publication in this journal is cited, in
accordance with accepted academic
practice. No use, distribution or
reproduction is permitted which does
not comply with these terms.

Impact of Iron oxide nanoparticles on sustainable production of biogas through anaerobic co-digestion of chicken waste and wastewater

Khalideh Al Bkoo Alrawashdeh^{1*}, Kamel K. Al-Zboon²,
Said Al Rabadi³, Eid Gul⁴, La'aly A. AL-Samrraie², Rabia Ali⁵ and
Jalal A. Al-Tabbal⁶

¹Mechanical Engineering Department, Al-Huson University College, Al-Balqa' Applied University, Irbid, Jordan, ²Water and Environmental Engineering Department, Al-Balqa' Applied University, Irbid, Jordan, ³Chemical Engineering Department, Al Balqa Applied University, Huson, Jordan, ⁴Biomass Research Centre, The University of Perugia, Perugia, Italy, ⁵Faculty of Pharmacy, University of Central Punjab, Lahore, Pakistan, ⁶Department of Applied Science, Al-Huson University College Al-Balqa' Applied University, Al-Huson, Jordan

As The effect of iron oxide nanoparticles (IONPs) on the anaerobic co-digestion (AD) of olive mill wastewater and chicken manure was investigated. In mesophilic conditions, biogas yield, methane (CH₄) content, the removal efficiency of TS, VS., acidification and hydrolysis percentage, and contaminant removal efficiency were investigated. Supplementing AD with IONPs at a concentration of 20 mg/g VS. > IONPs and INOPs >30 mg/g VS. causes an inhibitor impact on biogas, methane generation, and hydrolysis. Furthermore, implantation with 20–30 mg of IONPs/kg VS. has induced an equivalent favorable impact, with hydrolysis percentages reaching roughly 7.2%–15.1% compared to the control test, in addition to a 1.3%–4.2% enhancement in methane generation yield. The maximum acidification concentration after five days of the incubation of 1,084, 9,463, and 760 g/L was attained with IONPs dosages of 25, 30, and 20 mg/g VS., respectively, compared to 713 g/L obtained with the control test. The results have illustrated that supplementing AD with a specific concentration of IONPs (20–30 mg/g VS.) has a significant effect and enhances the inhibitor removal efficiency, most possibly due to the small surface area of IONP particles. The resultant increase in the active surface area enhances the enzyme diffusion within the substrate. This study provides new data specifying the enhancement of iron oxide nanoparticles (IONPs) and identifies the impact of IONP doses at various concentrations on the AD of olive mill wastewater and chicken waste.

KEYWORDS

anaerobic co-digestion (AcoD), iron oxide nanoparticles (Fe₂O₃), wastewater, chicken waste, biogas, sustainability

1 Introduction

The demand of renewable energies is rising and the policies of waste management that require the recycling of wastes, the anaerobic digestion (AD) process has been developed for treating a wide variety of organic wastes, including olive mill wastewater (OMWW) (Alrawashdehbkoor et al., 2020) and chicken manure (CM) (Jurgutis et al., 2020). The anaerobic co-digestion process is shown as a potential option for decreasing bio-waste development (Mouftahi et al., 2020). Additionally, the nature of the OMW and CM components needed a short residence time for efficient degradation (Oz and Uzun, 2015). It was also reported that the co-digestion increased the biogas yield by 22% (Azbar et al., 2008) and the removal of volatile solids (VS.) was in the range of 32% of the total solids (TS) (Liao et al., 2014).

In certain proportions, as mentioned in the literature, heavy metals with a size greater than nanoparticles' effects were investigated utilizing an anaerobic digestion process, absorption, and adsorption technology (Sajid et al., 2020; Dilshad et al., 2021; Al bkoor Alrawashdeh, 2022; Alrawashdeh et al., 2022; Sajid et al., 2022). The characteristics of nanostructured materials can be radically different from those of bulk materials or larger-scale entities. Therefore, nanomaterials have increased transportation in environmental media, and they have promising importance as different bioactive materials and technologies with novel activities for organisms. According to Huangfu et al. (2019) (Sajid et al., 2020), nanoparticles have an essential characteristic in biological system interaction because they can permeate cell membranes, allowing interaction with the immune system. Nanomaterials' particular qualities, such as large high reactivity, surface area, and high selectivity, allow them to have beneficial impacts (Sajid et al., 2020). Enzymatic adsorption onto NPs and heavy metals, on the other hand, will result in conformational changes, as well as inhibition or increase of enzyme activity based on quantity (Chen et al., 2017; Dilshad et al., 2021).

Recently, various studies have demonstrated that the addition of heavy metals (Alrawashdehbkoor et al., 2020) and conductive nanoparticles (NPs) has a favorable impact which increases the CH₄ production rate along with enhancement in AD process stability (Lee and Lee, 2019). Among the NPs, multi-compound, carbonaceous nanomaterials, the iron oxide nanoparticles (IONPs) that contain maghemite, magnetite, and hematite (Sekoai et al., 2019) and the nano-zero-valent-iron particles (NZVIPs) (Yang et al., 2013a) are employed to optimize the AD process. NZVIPs with considerable strong chemical reducibility and a high surface area have the most attractive uses in biodegradability processes relative to zero-valent metals (ZVMs) (Li et al., 2016). Yang et al. (2013b) revealed, on the other hand, that NZVIPs (55 nm) equivalent to 56 mg/L (1 mM) inhibited the methanogenesis of the AD

process by 20%. The study demonstrated that the inhibition was due to NZVIPs-induced cell 200 integrity degradation. Furthermore, in the presence of NZVIPs, Lowry and Reinhard (Lowry and Reinhard, 2001) showed an enhanced H₂ production in anaerobic conditions.

However, because of their magnetic properties and strong chemical stability, IONPs have a very high potential. IONPs have a particularly high potential due to their magnetic characteristics and their high chemical stability (Baek et al., 2018) and enhance the direct transfer of electrons during the AD process. Interspecies electron flow is achieved by direct transmission of electrons produced by electron-donating bacteria (EDB) to acceptors, methanogenic archaea that may convert CO₂ to CH₄ utilizing electrons supplied from the EDB via conductive materials (Sekoai et al., 2019). During the syntrophic metabolism, the enhancing behaviours of IONPs appear as a result of iron oxides working as conduits of electrons and accelerating direct interspecies electron flow without being shuttled by molecular hydrogen (Xu et al., 2019).

Early research focused on the influence of IONPs on the AD process, concentrating on syntrophic metabolism or syntrophic methanogenesis. According to a study conducted by Kato et al., (Kato et al., 2010), IONPs (which include hematite and magnetite) greatly enhance the rate and start-up time of production during the conversion from acetate to methanogenesis. Another research looked at CH₄ generation in the presence of IONPs (magnetite), and the results demonstrated that direct electron flow accelerates syntrophic methanogenesis (Zhang and Lu, 2016). Also, the influence of IONPs on the first (hydrolysis) and second (acidification) stages of the AD process as well as a methanogenic stage (Sajid et al., 2020). These studies revealed that IONPs has a significant impact on the solubility of complex organic substrate.

Despite the above-stated favourable benefits, IONPs can have inhibitory effects when used at high dosages. These inhibition effects can be attributed to the high catalytic conditions created at the IONP surface, which can immediately inhibit bacterial activity by causing significant destruction of the membrane surface and respiratory processes via reductive breakdown of enzymes' functional groups (Huang et al., 2016) and, presumably, to the accelerated hydrogen synthesis and concentration that result in the accumulation of volatile fatty acids (VFAs) (Lee et al., 2008). However, studies were conducted to assess IONPs at specific concentrations without identifying the level of promoting and inhibiting IONP supplementary doses during the anaerobic digestion process.

Therefore, this study was designed to investigate the best organic loading rate and enzymatic pre-treatment technique for mesophilic CO-digestion of CM: OMW to generate higher biogas and CH₄ content utilizing BMP tests at the first stage. Whereas the second stage aims to realize the potential beneficial impacts of magnetite IONPs on the AD process. This study investigates the effects of IONPs on the co-digestion of OMW and CM at various

TABLE 1 The characterization of AS and OMW.

Substrate	Moisture, U(%)	Total solide, TS (%)	Volatile solids, VS. (%)	Ash (%)	Fixed carbone (%)	pH	Phenols (mg ^l ⁻¹)	TCOD (g ^l ⁻¹)	BOD5 (g ^l ⁻¹)
CM	76.80 ± 0.22	23.20 ± 1.04	4.36 ± 0.41	0.04 ± 1.0	0 ± 0.55	6.13 ± 0.26	4.61 ± 0.79	8.56 ± 0.64	7.8 ± 0.81
OMW	93.65 ± 1.51	6.35 ± 1.91	2.50 ± 1.73	0.39 ± 1.08	18.79 ± 1.03	4.72 ± 0.47	6.7 ± 1.13	55.2 ± 2.18	9.47 ± 0.03
Inoculum	98.56 ± 0.52	1.44 ± 0.23	0.43 ± 0.02	0.50 ± 0.31	0.51	6.53 ± 1.05	3.02 ± 0.41	17.23 ± 3.73	2.71 ± 3.59

doses. In addition, this study aims to investigate the impact of IONP doses on biogas and methane production, reduction of TS, VS., COD, colour, turbidity, and process stability.

2 Methodology—Materials and method

2.1 Feedstock

The CM substrate was obtained from a local chicken layer farm in Irbid, Jordan. At the same time, the OMW substrate was collected from the three-phase oil extraction station for the 2021 olive harvest season. Both CM and OMW feedstocks were kept at 4°C until they were used. The inoculum was prepared from previous AD tests, which were conducted on cow waste.

According to UNI 5667–13/2000, all the substrates of OMW, CM, and inoculum were prepared to be used in AD tests, as described by Alrawashdeh et al. (2017). The characteristics of physicochemical and proximate analysis of substrates were determined by utilizing a thermogravimetric analyzer (TGA 701, LECO, St. Joseph, MI, United States). The analyses included volatile solid (VS.), total solid (TS), humidity (U), ASH, and fixed carbon (F.C), as reported in (Al bkoor Alrawashdeh, 2018; Alrawashdeh and Al-Essa, 2020). Table 1 summarizes the characteristics of the co-substrate and inoculum. The pH of substrates was measured by using a pH meter.

The concentration of Fe was measured by atomic absorption spectroscopy with flame atomization (AAS-FA) using a Perkin Elmer analyzer 400 spectrometer (CT, Norwalk, United States), and the extractable Fe was determined using the Mehlich 3 technique (Nduwamungu et al., 2009; Al bkoor Alrawashdeh et al., 2017; Goulding et al., 2020). A carbon analyzer (LECO CR-412, United States) was used to determine total carbon (C) in substrates, and the Kjeldahl method was used to estimate total nitrogen (TKN), which presents the total concentration of organic ammonia and nitrogen (Goulding et al., 2020). The C/N ratio of the CM and OMW was 8.52 ± 2.46 and 38.56 ± 4.09 , respectively. Where the desirable ratio of C/N is in the range of 20–30,

this range can be achieved by co-digestion of substrates of CM and OMW at a specific ratio. The Fe concentration of CM and OMW was 132.4 ± 0.77 mg/kg and 34.06 ± 1.68 mg/kg, respectively.

Methods 2320B, 4,500, 3,125, 4,500- P, and 4,500- NH₃ from the Standard Methods for the Examination of Water and Wastewater (Baird et al., 2017) were used to measure the phosphorus and ammonia. To determine VFAs, the GC-FID was used according to the method reported by Boe et al. (2007).

2.2 Iron oxide nanoparticles preparation

IONPs (magnetic) were synthesized by utilizing chemical and physical methods by dissolving two moles of FeCl₃·6H₂O (ferric-molecular weight 270.33) and one mole of FeCl₂·4H₂O (ferrous-molecular weight 198.81) into 100 ml of deoxygenated water separately. Simultaneously, 0.64 mole of NaOH were prepared and dissolved in 750 ml of deoxygenated water, and the NaOH was put on a hot plate at a temperature of 60–75 °C with a magnetic stirrer. After that, ferric and ferrous were mixed for 5 min. Both ferric and ferrous (after mixing them for 30 min) were poured dropwise into NaOH and mixed together. Afterward, the magnetic nanoparticle (Fe₃O₄) appeared in black. The initial pH of the mixture was 12, then decreased until the pH value reached an optimum value of 7. The synthesized magnetic nanoparticles were washed using 25% distilled water and 75% ethanol with a continuously measured pH value. Finally, the prepared nanoparticles were collected and dried using an electrical oven (40–45°C) for 24 h. In the last stage, the synthesized nanoparticles were ground to a suitable dimension (40–78 nm in width and 70–100 nm in length).

2.3 Experimental setup

The investigation tests were carried out in two stages; the first stage was performed with various CM/OMW substrates' ratios in order to specify the optimum ratio for high AD stability, biogas, and methane production. The second stage was to identify and investigate the influence of IONPs supplementary doses on the

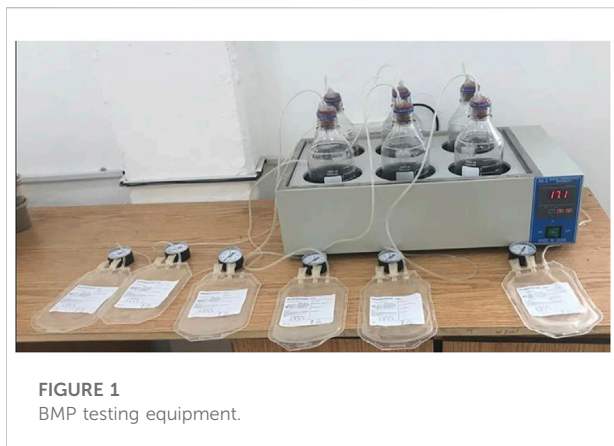


FIGURE 1
BMP testing equipment.

co-digestion process. Various parameters were investigated to identify the optimum supplementary doses of IONPs in terms of digestion stability, retention time, methane content, and biogas yield. Pressure and temperature were used to estimate daily biogas production. A gas chromatograph (490 micro-GC, Agilent Technologies, Santa Clara, CA, United States) was used to analyze biogas. Argon and helium were employed as carrier gases at a 10 ml/min flow rate. The detector injector and columns were heated to 180, 100, and 80°C, respectively. Excess biogas was regularly vented to avoid pressure situations and the risk of explosion (Al bkoor Alrawashdeh, 2018; Alrawashdeh and Al-Essa, 2020). contains a detailed explanation of the laboratory equipment.

The hydrolysis percent was calculated by Eq. 1 based on Kassab et al. (2020), which is related to the soluble COD relative to an initial concentration of COD.

$$\text{Hydrolysis} = \frac{\text{COD}_{\text{CH}_4(t)} + \text{COD}_{\text{S}(t)} - \text{COD}_{\text{S}(0)}}{\text{COD}_{\text{th-in}} - \text{COD}_{\text{S}(0)}} \times 100\% \quad (1)$$

Where the $\text{COD}_{\text{CH}_4(t)}$ is the COD equivalent of CH_4 generated during any time (t), $\text{COD}_{\text{S}(t)}$ is the soluble COD during any time, $\text{COD}_{\text{S}(0)}$ is the soluble COD at $t = 0$, and $\text{COD}_{\text{th-in}}$ is the initial theoretical COD. The $\text{COD}_{\text{th-in}}$ can be obtained using the stoichiometric analysis of the reaction of substrate oxidation (Kassab et al., 2020).

The acidification percent can be calculated using Eq. 2, and was assessed based on the percent of the VFA equivalent COD at a specific time ($\text{COD}_{\text{VFA}(t)}$), the VFA equivalent COD at time $t = 0$ acidified COD ($\text{COD}_{\text{VFA}(0)}$) relative to the $\text{COD}_{\text{th-in}}$.

$$\text{Hydrolysis} = \frac{\text{COD}_{\text{CH}_4(t)} + \text{COD}_{\text{VFA}(t)} - \text{COD}_{\text{VFA}(0)}}{\text{COD}_{\text{th-in}}} \times 100\% \quad (2)$$

TABLE 2 Concentration of the IONPs utilized in the AD process tests.

Test code	IONP concentration (mg/gVS)
Control	0
IONP ₁₅	15
IONP ₂₀	20
IONP ₂₅	25
IONP ₃₀	30
IONP ₃₅	35
IONP ₄₀	40

2.3.1 The first stage: Specify the optimum ratio of CW: OMW

Biochemical methane potential (BMP) tests were carried out in duplicates at $40 \pm 2^\circ\text{C}$ (mesophilic conditions). The BMP test was performed in a vessel of 1 L conducted with one primary outlet closed with a stopper with two holes; one for collecting samples and controlling the pH value, and the other for allowing the generated biogas to pass through, as shown in Figure 1.

Each vessel was connected with a gas sampling bag (0.5 L), which has a septum fitting for syringe sampling and an emptying tube. In addition, each bag is connected to a pressure gauge; also, a thermocouple was used to measure the gas temperature to calculate the daily biogas production.

The ratio concentrations of CW to OMW by weight were: 25:75, 50:50, 75:25 (v/v), 100% of CW, and 100% OMW in weight respectively. The quantities of substrate added were prepared according to Alrawashdeh et al. (Al bkoor Alrawashdeh et al., 2017). All vessels were tightly closed and flushed with N_2 to remove oxygen. As shown in Figure 1, the vessels were immersed in a thermostatic bath in mesophilic conditions ($40 \pm 0.2^\circ\text{C}$). During the first two weeks of the test period, all the vessels were manually shaken twice a day (for 1 min) as recommended by the reference (Al-Juhaimi et al., 2014). In order to ensure that the microorganism and substrate can interact and to prevent the formation of buffer accumulation.

Each reactor was filled with up to 20% of its volume with different mixtures of OMW-CM and the inoculum (Al bkoor Alrawashdeh et al., 2017; Al bkoor Alrawashdeh, 2018). After loading the vessels, the initial pH of substrates was adjusted to around 7.3 ± 0.5 by adding 1.0 ml of KOH. Due to high acidity, each vessel was corrected by adding the same quantity of KOH every 3 days. For BMP tests, at least 30 days were required before the biogas produced less than 1% of the total biogas accumulation up to that point (Agarbaty et al., 2022).

2.3.2 The second stage: The influence of iron oxide nanoparticles on the anaerobic co-digestion process

With and without the addition of IONPs, each bioreactor was filled with the optimal ratio of CM to OMW substrate. To achieve the necessary nanoparticle concentrations, different aliquots of IONPs stock solutions were added. BMP tests were conducted with magnetite IONP concentrations of 15, 20, 25, 30, 35, 40 mg IONPs/g VS. (see table 2). To achieve AD conditions, the reactors were flushed with N₂ for 2 min after being loaded.

After that, all vessels were immersed in a bath of thermostatic water set to mesophilic conditions of 40°C ± 0.2 and ran at an HRT of 40 days. To assess the influence of magnetic IONPs on the AD process, biogas production was measured in volume on the daily basis. The biogas produced was analyzed to determine the CH₄ content. Also, the effluents were analyzed to investigate the percentage of VS., TCOD, BOD₅, and phenols removal efficiency.

3 Results

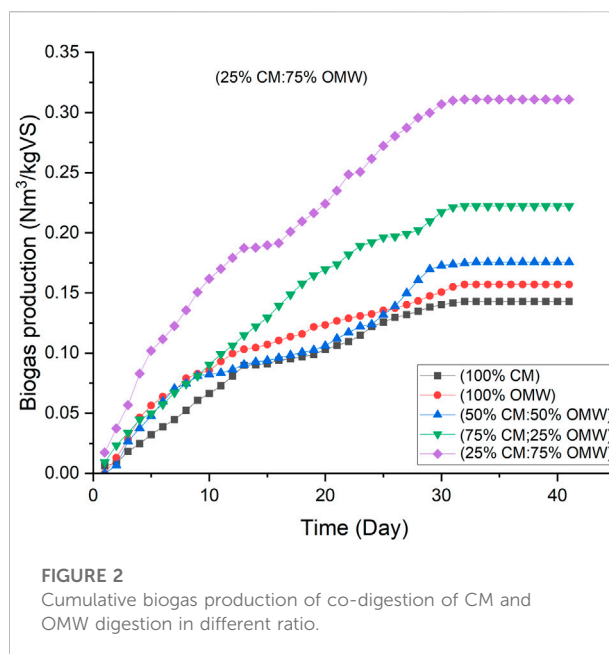
3.1 Optimum ratio of CM:OMW

In comparison to the typical values published in the literature, the measured pH of the CM (6.13 ± 0.26) is indeed low. The CM pH was reported to be 7.5 by Kucuker et al. (2020). During the storage period, it appears that acidification had already begun. While pH (5.72 ± 0.47) of OMW is lies within the range reported in the literature (Alrawashdehbkoor et al., 2020). However, the acidity of the mixture required readjusting the pH in proportion to the conditions of the AD process, as mentioned previously.

The VS./TS ratio was 51.51%, 49.24%, 47.83%, 46.88% and 55.8 of 25:75, 50:50, 75:25 (v/v), 100% of CM, and 100% of OMW, respectively. VS./TS ratio of all mixtures highlights the high organically. However, among the co-digestion substrates, the low level of soluble TCOD reveals the predominance of granular COD in the co-substrate at the ratio of 75:25 (CM: OMW) and 100% of mono-digestion of OMW specifically, which might slow down degradation related to a limitation in hydrolysis.

The C/N ratio of 75:25 CM: OMW and 100% CM was below the typically desirable limit of 20–30 for an effective AD process (Zhang et al., 2014), whereas the C/N ratio of 100% OMW (180 g of OMW and 20 g of inoculum) was higher than desirable ratio (36.34). Furthermore, upon co-digestion, 25:75 and 50:50 (CM: OMW) were generally characterized by a suitable C/N ratio (29.57 and 22.80). However, many studies have reported that co-digestion may be done satisfactorily with C/N ratios in the range of 8.8–13 (Koch et al., 2016).

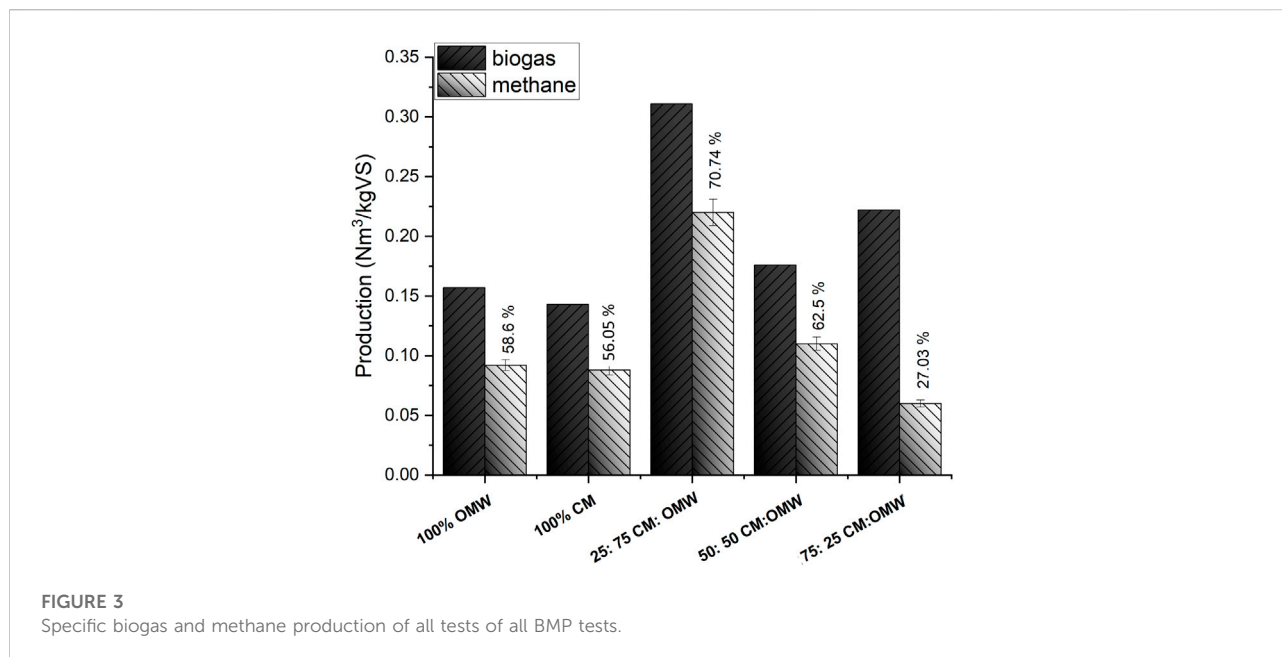
The synthetic mixture of 25:75, 50:50, 75:25 (v/v), 100% CM, and 100% OMW had a COD:N:P ratio close to, 316:5:1.1, 355:5:



0.9, 300:22:4.4, 170:5:1, and 908:5:1.8, respectively. Hence, in the nutrient supplementation context, the comparison of each mixture's determined COD:N:P ratio with what has been reported in the literature for a stable and successful AD process (300:5:1) (Park et al., 2018). Also, for the AD process, a COD:N:P ratio of 250:5:1 is recommended (Hamza et al., 2016; Leite et al., 2017; Park et al., 2018; Baniamerian et al., 2019), but there is considerable variance between 900:5:1.7 and 150:5:1 (Bashaar, 2004; Araujo et al., 2008). It is worth noting that "N" in this context refers to total nitrogen (Hussain and Dubey, 2013). That confirms the phosphorous deficiency than the recommended value in 50:50, 75:25 of CM:OMW which is typically recommended for AD and production of biogas (Leite et al., 2017).

The test's duration is about 42 days to complete the stability. The pH of each vessel declined dramatically during start-up, reaching high acid values; pH control improved the production rate of the co-digestion 75:25, 25:75, and 50:50 of CM:OMW, while mono-digestion of 100% OMW and 100% CM remained relatively stable. To follow organic matter decomposition, total and volatile solids were measured after the last day of the AD process. Both co-digestion and mono-digestion decomposition rates vary depending on the ratio of CM and OMW substrates.

Figure 2 shows the cumulative biogas production of all tests, whereas Figure 3 shows the specific biogas and methane (CH₄) content. Daily production of tests 25:75 CM:OMW, 50:50 CM: OMW, and 75:25 CM:OMW show similar tendencies. A low-production-rate phase is followed by a high-production-rate phase until a plateau is attained, which is then maintained in



the last declining phase. However, the biodegradation and performance of the substrate of 25:75 CM:OMW is higher than the others. A delayed acidogenic phase is found in co-digestion tests, according to the biodegradation of 100% of CM and OMW (Figure 3). Methane content, as shown in Figure 4, was affected by the C/N ratio and COD:N:P. Despite the high biogas generation (75:25 CM: OMW), the methane concentration was extremely low (27.03%). This had an impact on methane generation, which was assessed by μ GC in the range of 58.6%–56.05% volume of biogas for mono-digestion tests. Overall, biogas and methane yield of 25:75 CM: OMW is much greater than that of 100 % CM and OMW mono-digestion and the other co-digestion (see Figures 2, 3). Following Sounni et al. (2017), this test was conducted using a low buffering capacity and a balanced process for tests of 25:75 CM: OMW and 50:50 CM:OMW.

3.2 Influence of iron oxide nanoparticles on the anaerobic co-digestion process

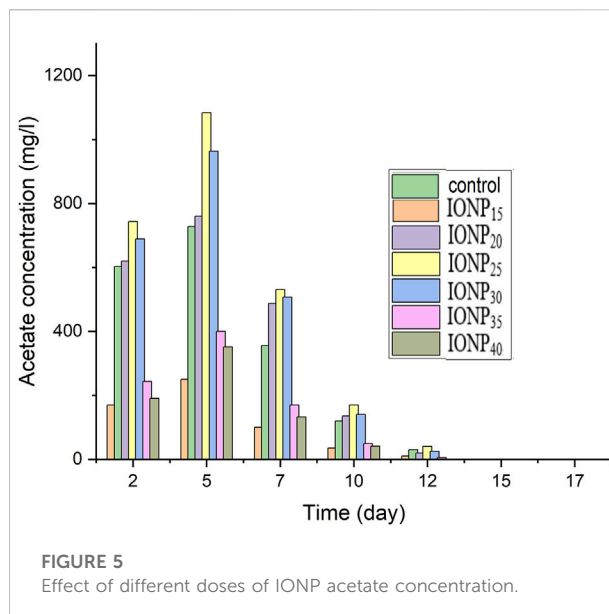
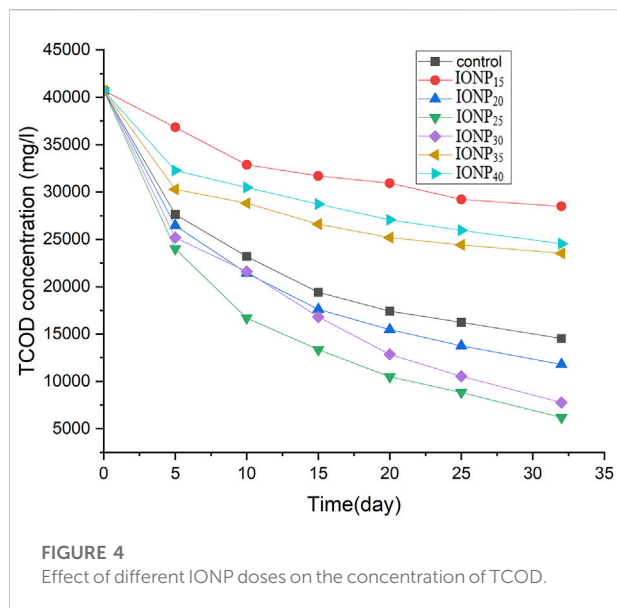
The identical technique used in the first stage of this study was used to conduct BMP testing. According to Al bkoor Alrawashdeh et al. (2017), the requisite inoculum was supplied, and the quantities of inoculum were calculated using the ratio of a co-substrate to inoculum 1.0 kg COD substrate/kg VS. inoculum. The co-substrate, which comprised of CM and OMW, was added at a 25:75 (CM: OMW) ratio, which was obtained based on the findings of the first stage of this research. Prepared IONPs were added to co-substrate at different

concentration 15, 20, 25, 30, 35, 40 mg IONPs/g VS. of substrate. All vessels were immersed in a thermostatic water bath at $40^{\circ}\text{C} \pm 0.2$ and operated at HRT for 30 days. Daily biogas production.

3.2.1 Effects of iron oxide nanoparticles on the hydrolysis

The effect of IONPs on TCOD reduction was evaluated since hydrolysis is significant in the kinetics of AD and is generally the rate-limiting phase. IONP concentrations of 15–40 mg IONPs/g VS. of substrate were employed in AD tests. The results (Figure 5) reveal that the greatest removal of TCOD attained in the control incubation was 26,166.9 mg/L (TCOD concentration of effluent is 14,528.12 mg/L), and after five days incubation period, it was 27,631.91 mg/L.

Figure 4 shows that the AD tests with the addition of IONPs achieved maximum reduction of TCOD concentrations of 34,509.36, 32,922.25, 28,893.45, 17,173.29, 16,725.65 and 12,208.5 mg/L according to TCOD concentration of effluent (mg/L) is 6,185.64, 7,772.745, 11,801.55, 23,521.71, 24,539.09 and 28,486.5 for IONP25, IONP30, IONP20, IONP35, IONP40, and IONP15, respectively. The test with an additional dose of IONP25 achieved the highest removal efficiency of TCOD (TCODre-eff). The peak values were reached after the first five days for all the test incubations of the IONP doses, where the IONP25 reached 41.1% of TCOD re-eff. Peak values were reached after five days with cumulative CH₄ production of 0.09, 0.076, 0.070, 0.051, 0.028, and 0.022 Nm³ CH₄/kg VS. for IONP doses of 25, 30, 20, 35, 40, and 15 mg IONPs/g VS., respectively, and for the same



incubation period, the control test reached 0.064 Nm³ CH₄/kg VS. As a result, the hydrolysis percentages reached after five days were estimated to evaluate whether elevated soluble TCOD in IONPs modified tests was related to the accumulation of soluble TCOD as a result of a decreased rate of consumption by methanogens or attributed to enhanced hydrolysis. The results revealed that the tests incubated with IONP25, IONP30, IONP20, IONP35, IONP40, and IONP15 achieved hydrolysis percentages of 85.3%, 81.5%, 79.3%, 77.4%, 62.9%, and 61.3%, respectively, compared to the control test's hydrolysis percentage of 70.2%. As a result, we came to the conclusion that IONPs had an enhancing effect on hydrolysis at specific concentrations. However, the results show that the doses of 30 mg/gVS \geq IONPs \geq 20 mg/gVS improve the hydrolysis percentage.

Several studies have extensively reported on the beneficial effects of magnetite on the hydrolysis process. Also, with an NP magnetite (diameter of 0.2 μ m) dose of 10 g/L, Zhao et al. (2018) observed a major increase (doubled) in active sludge protein hydrolysis and an increase in the activity of enzymes, respectively. Furthermore, 1 g/L magnetite NPs achieved an increase in the total polysaccharide degradation by 15.8% (Gou et al., 2014).

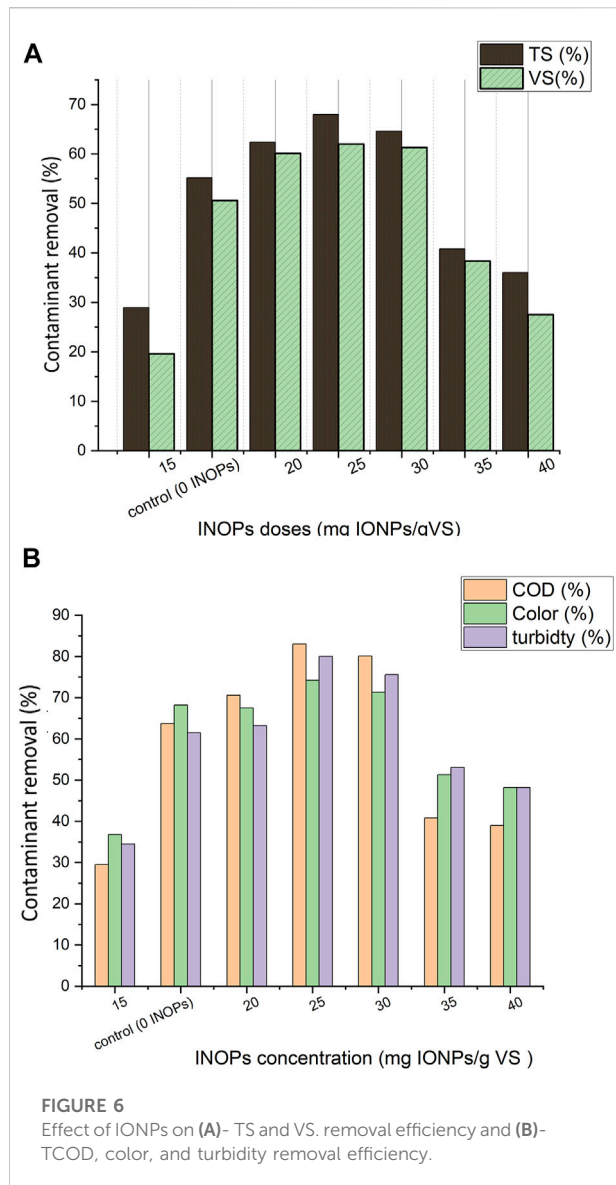
3.2.2 Effects of iron oxide nanoparticles on the acidification

The CH₄ content is linked to the VFAs production during acidification of the substrate. The effect of IONPs on the VFAs' availability for methanogenesis was investigated. As shown in Figure 5, the acetate production was strongly stimulated, with a maximum concentration (within 5 days) of 1,084, 9,463, 760, 400, 351, and 250 mg/L by IONP25, IONP30, IONP20, IONP35, IONP40, and IONP15, respectively, compared to the VFAs

concentration of the control test 713 mg/L. Mechanism exploration exhibited that the main reason for the enhanced VFAs accumulation in the presence of a specific concentration of IONP was that more acetic acid was generated during the acidification of substrate, which was increased significantly. This result reinforces what was found in the previous section about the rate of decomposition.

This result reinforces what was found in the previous section of the study related to the decomposition rate. This contradicts some studies (Su et al., 2013; Al-Juhaimi et al., 2014; Gou et al., 2014; Kim et al., 2016; Baiju et al., 2018; Zhao et al., 2018; Zhang et al., 2019; Wu et al., 2020) which reported that any increase in magnetic nanoparticles enhances both acidification and establishing.

Acetate is the most common component of VFAs, which can be employed as a carbon source for eliminating phosphorus and nitrogen from the organic waste substrate (Su et al., 2013; Kim et al., 2016; Baiju et al., 2018; Zhang et al., 2019; Wu et al., 2020). The synthesis of short-chain VFAs was responsible for more than 80% of the soluble COD produced. VFA generation was also impacted by pH, with alkaline circumstances producing substantially more VFA. The TS can be converted anaerobically into VFA throughout the digestive phase. The tests with IONP dosages \geq 35 mg IONPs/g VS. and IONP dosages < 20 mg IONPs/g VS. were characterized by low gradeability, and lower yield was achieved at higher TS concentrations (high organic load), most likely due to inhibition at high VFA concentration. Using synthesized VFA, batch growth under nitrogen limitation resulted in greater lipid formation. The results obtained are in agreement with the studies that reported acceleration of the hydrolysis and acidification, and



solubilization of the substrate with the addition of nanoparticles of iron oxidize (Baiju et al., 2018; Zhang et al., 2019; Wu et al., 2020). According to Peng et al. (2018b), the addition of magnetite and granular activated carbon to an AD at the same time increased sludge hydrolysis and methane production, resulting in improved digestion of the sludge.

3.2.3 Effects of iron oxide nanoparticles on the biological treatment

The chemical and physical features of the IONP additions aided the bacterial community's enzymatic activity for biogas and methane generation as well as the catalytic enhancement of substrate treatability efficiency in the AD process. Figures 4, 6A,B show the results of contaminant removal from the substrate after a 32-days HRT and a mesophilic temperature of $40 \pm 2^\circ\text{C}$.

Stimulatingly, considerable differences were noticed for the TS and VS. removal (Figure 6A). Surprisingly, the removal effectiveness of TS and VS. was found to be IONP25 > IONP30 > control > IONP20 > IONP35 > IONP40 > and IONP15, respectively. These findings are consistent with previous research, which found that specific concentrations of iron-based additives have accelerated substrate deterioration in bioreactors. IONPs also acted as either separator or as reaction media with a wide surface for adsorption and aggregation of the pollutants.

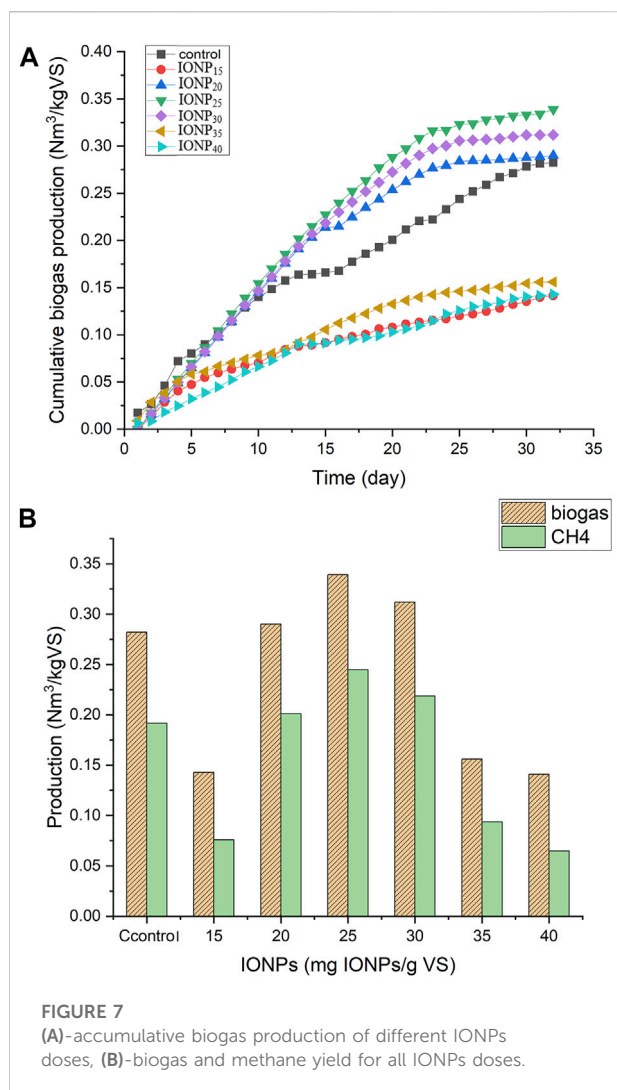
The bioreactor efficiency was measured using the percent of COD removal, color and turbidity, and the other aforementioned criteria. Removal efficiency of COD (Figures 4,6) were determined to be IONP25 (84.8%) > IONP30 (80.9%) > IONP20 (71%) > control (64.3%) > IONP35 (42.2%), IONP4 (39.7%) and IONP15 (30%), respectively. Also, Figure 6B shows that in the terms of colour removal efficiency, an increase order was identified as IONP25 (74%) > IONP30 (72.8%) > IONP20 (67.9%) > control "0 IONP" (69%) > IONP35 (52.9%), IONP40 (48.8%) and IONP15 (36.9%), respectively.

Contains 25 mg IONP/gVS and a bio augmenting mixture (25:75 CM:OMW). This confirms that metal-based oxides' catalytic and enzymatic abilities aided biodegradation when compared to a control reactor (no additives) (Mu et al., 2011b; Peeters et al., 2016; Suanon et al., 2016; Baiju et al., 2018; Er et al., 2018; Wu et al., 2020). This conclusion is consistent with recent research (Peeters et al., 2016; Baiju et al., 2018), which found that bioaugmentation of organic fraction waste treatment at a certain level enhanced the removal efficiency of pollutants compared to non-bioaugmented reactors. Also, the results confirmed with studies reported that in the AD process, IONP additions might reduce the lag phase of the bioreactor while increasing treatment efficiency (Bashaar, 2004).

3.2.4 Effects of iron oxide nanoparticles on the biogas production

In comparison to the control (0 additive), Figure 7A,B show the effects of IONPs on cumulative biogas generation and methane content at various concentrations. The cumulative biogas obtained in ascending order are IONP25 (0.339 Nm³/kgVS) > IONP30 (0.312 Nm³/kgVS) > IONP20 (0.312 Nm³/kgVS) > control (0.282 Nm³/kgVS) > IONP35 (0.156 Nm³/kgVS) > IONP40 (0.143Nm³/kgVS) > IONP15 (0.141 Nm³/kgVS). The highest biogas production was observed from the 5th to the 22nd day, after which there was a daily drop-in generation rate until the 32nd day, when the experiment was terminated.

Interestingly, the control test's daily biogas surpassed the reactor with 35 mg/g VS. > IONPs addition >15 mg/g VS As a result, a specific concentration of metal based IONPs may have inhibited or poisoned the microorganisms in the reactor, causing them to perform poorly (Er et al., 2018). This improved the way



biogas was produced in relation to the methanogenic activity's reaction. Even though biogas generation dropped dramatically in the IONP35, IONP40, and IONP15 reactors, the decline occurred at various periods. The stimulating effects of IONPs on methanogen cell attachment and metabolic co-enzymes required for the hydrolysis, acidification, and methanation stages of AD for biogas generation (Mu et al., 2011b; Suanon et al., 2016; Er et al., 2018) might explain this phenomenon. IONPs have a substantial effect on the activation and binding of microbe receptors for methanogenesis and consequent nutritional enrichment, according to Suanon et al. (2016). Mu et al. (2011b) also claim that the IONP additions increased biogas and CH₄ generation, which is consistent with the findings of this study.

Figure 7B illustrates that the addition of IONPs had a favorable impact not only on the biogas yield but also on the efficiency of the biogas composition as a percentage of CH₄. All of the bioaugmented tests 30 mg/g VS. > IONP>20 mg/g

VS. had a high CH₄ yield. The highest methane production was achieved by IONP25. The soluble COD, which was accessible to the methanogens consortia participating in the degradation, can be connected to methane generation (Métivier et al., 2020).

4 Conclusion

The optimum ratio of co-digestion of chicken manure and olive mill waste was investigated in terms of biogas and methane production, stability, and removal efficiency of TCOD, VS., and TS. The results show that the ratio of 25:75 CM:OMW is the best composition of co-substrate. The co-substrate is conducted to investigate the impact of iron oxide nanoparticles (IONPs) at different concentrations on the performance of the AD process.

In this study, the influence of adding a specific concentration of IONPs to improve the AD process of co-digestion of CM:OMW into bioenergy was shown to be extremely promising and a realistic technique for organic waste management.

The augmentation of the IONPs with 20–30 mg/g VS. resulted in improved 6.7%–20.5%, 3%–15.4%, 1.8%–6.1%, 6.3%–12.5%, and 9.9%–12.3% compared to the control test (0 additives) treatability performance (COD, turbidity, color, TS, and VS. removal efficiency). From the results obtained over the operating hydraulic retention time of 32 days, the addition of 25 mg IONPs/g VS. showed stable performance with the highest biogas yield (0.339 Nm³/kg VS.) and methane content of 72.2%. The results show that supplementing AD tests with IONPs at doses of 20–35 mg/g VS. resulted in a considerable rise in hydrolysis percentages to 85.3%–77.4%, compared to 70.2% in the control test. Acidification was also greatly enhanced, with acetate being the most prevalent VFA. In tests incubated with IONP concentrations of 20, 30, and 25 mg/g VS., respectively, acidification percentages reached %, 80.9%, and 84.8%, compared to just 64.3% in the control incubation.

Data availability statement

The original contributions presented in the study are included in the article/supplementary material, further inquiries can be directed to the corresponding author.

Author contributions

The author KA, the executor and designer of the campaign, wrote the paper and elaborated on the data, also, biogas process. RA analyzed the heavy Metals behavior, and BMP analysis. KA-Z conducted experiments,

prepare a framework. LA-S reviewed and data analysis. The author EG prepared and analyzed data, results analysis, and review. SAR and JA-T editing according to the reviewer comments.

Acknowledgments

This author acknowledges the contributions and guidance of colleagues, and sincere gratitude to the Al-Balqa' Applied University (Cooperative action in recycling and reuse of olive mill waste for food and agriculture production-INT/20/K18), and Biomass Research Centre Perugia University for their support and providing the facilities to conduct this research work.

References

- Agarbati, A., Canonico, L., Comitini, F., and Ciani, M. (2022). Ecological distribution and oenological characterization of native *Saccharomyces cerevisiae* in an organic winery. *Fermentation* 8 (5), 224. doi:10.3390/fermentation8050224
- Al bkoor Alrawashdeh, K. (2022). Anaerobic Co-digestion efficiency under the stress exerted by different heavy metals concentration: An energy nexus analysis. *Energy Nexus* 7, 100099. doi:10.1016/j.nexus.2022.100099
- Al bkoor Alrawashdeh, K. (2018). Improving anaerobic Co-digestion of sewage sludge with thermal dried olive mill wastewater. *Waste Biomass Valorization* 10 (8), 2213–2219. doi:10.1007/s12649-018-0234-9
- Al bkoor Alrawashdeh, K., Pugliese, A., Slopicka, K., Pistolesi, V., Massoli, S., Bartocci, P., et al. (2017). Codigestion of untreated and treated sewage sludge with the organic fraction of municipal solid wastes. *Fermentation* 3 (3), 35. doi:10.3390/fermentation3030035
- Al-Juhaimi, F. Y., Hamad, S. H., Al-Ahaideb, I. S., Al-Otaibi, M. M., Ghafoor, K., Abbasi, T., et al. (2014). Biogas production through the anaerobic digestion of date palm tree wastes - process optimization. *BioResources* 9 (2). doi:10.15376/biores.9.2.3323-3333
- Alrawashdeh, K. A. B., Slopicka, K., Alshorman, A. A., Bartocci, P., and Fantozzi, F. (2017). Pyrolytic degradation of olive waste residue (OWR) by TGA: Thermal decomposition behavior and kinetic study. *J. Energy Power Eng.* 11 (8). doi:10.17265/1934-8975/2017.08.001
- Alrawashdeh, K. A. B., and Al-Essa, A. H. (2020). Anaerobic Co-digestion mill wastewater—activated sludge effect of aerobic pretreatment on the performance of OMW anaerobic digestion. *Waste Biomass Valorization* 11 (9), 4781–4788. doi:10.1007/s12649-019-00785-9
- Alrawashdeh, K. A. B., Al-Samrri, L. A., Al Issa, H. A., Qasem, I., Hussien, A. A., Al-Zboon, K. K., et al. (2022). Prediction and optimization of biogas production from OMW digestion using fenton pre-treatment process with particle swarm optimization. *Int. J. Des. Nat. Ecodyn.* 17 (2), 157–168. doi:10.18280/ijndne.170201
- Alrawashdehbkoor, K. A., Gul, E., Yang, Q., Yang, H., Bartocci, P., and Fantozzi, F. (2020). Effect of heavy metals in the performance of anaerobic digestion of olive mill waste. *Processes* 8 (9), 1146. doi:10.3390/pr8091146
- Araujo, D. J., Rocha, S. M. S., Cammarota, M. C., Xavier, A. M. F., and Cardoso, V. L. (2008). Anaerobic treatment of wastewater from the household and personal products industry in a hybrid bioreactor. *Braz. J. Chem. Eng.* 25 (3), 443–451. doi:10.1590/S0104-66322008000300002
- Azbar, N., Keskin, T., and Yuruyen, A. (2008). Enhancement of biogas production from olive mill effluent (OME) by co-digestion. *Biomass Bioenergy* 32 (12), 1195–1201. doi:10.1016/j.biombioe.2008.03.002
- Baek, G., Kim, J., Kim, J., and Lee, C. (2018). Role and potential of direct interspecies electron transfer in anaerobic digestion. *Energies* 11, 107. doi:10.3390/en11010107
- Baiju, A., Gandhimathi, R., Ramesh, S. T., and Nidheesh, P. V. (2018). Combined heterogeneous Electro-Fenton and biological process for the treatment of stabilized landfill leachate. *J. Environ. Manag.* 210, 328–337. doi:10.1016/j.jenvman.2018.01.019
- Baird, R. B., Eaton, A. D., and Rice, E. W. (2017). *Apha-American public health association. Standard methods for the examination of water and wastewater.* 23rd Edn. Washington, D.C.: American Public Health Association, American Water Works Association, Water Environment Federation
- Baniamerian, H., Isfahani, P. G., Tsapekos, P., Alvarado-Morales, M., Shahrokhi, M., Vossoughi, M., et al. (2019). Application of nano-structured materials in anaerobic digestion: Current status and perspectives. *Chemosphere* 229 (12), 188–199. doi:10.1016/j.chemosphere.2019.04.193
- Bashaar, Y. A. (2004). Nutrients requirements in biological industrial wastewater treatment. *Afr. J. Biotechnol.* 3 (4), 236–238. doi:10.5897/ajb2004.000-2042
- Boe, K., Batstone, D. J., and Angelidaki, I. (2007). An innovative online VFA monitoring system for the anaerobic process, based on headspace gas chromatography. *Biotechnol. Bioeng.* 96 (4), 712–721. doi:10.1002/bit.21131
- Chen, M., Zeng, G., Xu, P., Lai, C., and Tang, L. (2017). How do enzymes 'meet' nanoparticles and nanomaterials? *Trends Biochem. Sci.* 42 (11), 914–930. doi:10.1016/j.tibs.2017.08.008
- Dilshad, M. R., Islam, A., Haider, B., Sajid, M., Ijaz, A., Khan, R. U., et al. (2021). Effect of silica nanoparticles on carbon dioxide separation performances of PVA/PEG cross-linked membranes. *Chem. Pap.* 75 (7), 3131–3153. doi:10.1007/s11696-020-01486-7
- Er, X. Y., Seow, T. W., Lim, C. K., and Ibrahim, Z. (2018). Natural attenuation, biostimulation and bioaugmentation of landfill leachate management. *IOP Conf. Ser. Earth Environ. Sci.* 140, 012034. doi:10.1088/1755-1315/140/1/012034
- Gou, C., Yang, Z., Huang, J., Wang, H., Xu, H., and Wang, L. (2014). Effects of temperature and organic loading rate on the performance and microbial community of anaerobic co-digestion of waste activated sludge and food waste. *Chemosphere* 105, 146–151. doi:10.1016/j.chemosphere.2014.01.018
- Goulding, D. A., Fox, P. F., and O'Mahony, J. A. (2020). Milk proteins: An overview. *Milk. Proteins* 1 (1), 21–98. doi:10.1016/b978-0-12-815251-5.00002-5
- Hamza, R. A., Iorhemen, O. T., and Tay, J. H. (2016). Anaerobic-aerobic granular system for high-strength wastewater treatment in lagoons. *Adv. Environ. Res.* 5 (3), 169–178. doi:10.12989/aer.2016.5.3.169
- Huang, Y.-X., Guo, J., Zhang, C., and Hu, Z. (2016). Hydrogen production from the dissolution of nano zero valent iron and its effect on anaerobic digestion. *Water Res.* 88, 475–480. doi:10.1016/j.watres.2015.10.028
- Huangfu, X., Xu, Y., Liu, C., He, Q., Ma, J., Ma, C., et al. (2019). A review on the interactions between engineered nanoparticles with extracellular and intracellular polymeric substances from wastewater treatment aggregates. *Chemosphere* 219, 766–783. doi:10.1016/j.chemosphere.2018.12.044
- Hussain, A., and Dubey, S. K. (2013). Specific methanogenic activity test for anaerobic treatment of phenolic wastewater. *Desalination Water Treat.* 52 (37–39), 7015–7025. doi:10.1080/19443994.2013.823116
- Jurgutis, L., Slepeliene, A., Volungevicius, J., and Amaleviciute-Volunge, K. (2020). Biogas production from chicken manure at different organic loading rates in a mesophilic full scale anaerobic digestion plant. *Biomass Bioenergy* 141, 105693. doi:10.1016/j.biombioe.2020.105693

Conflict of interest

The authors declare that the research was conducted in the absence of any commercial or financial relationships that could be construed as a potential conflict of interest.

Publisher's note

All claims expressed in this article are solely those of the authors and do not necessarily represent those of their affiliated organizations, or those of the publisher, the editors and the reviewers. Any product that may be evaluated in this article, or claim that may be made by its manufacturer, is not guaranteed or endorsed by the publisher.

- Kato, S., Nakamura, R., Kai, F., Watanabe, K., and Hashimoto, K. (2010). Respiratory interactions of soil bacteria with (semi)conductive iron-oxide minerals. *Environ. Microbiol.* 12 (12), 3114–3123. doi:10.1111/j.1462-2920.2010.02284.x
- Kassab, G., Khater, D., Odeh, F., Shatanawi, K., Halalshah, M., Arafah, M., et al. (2020). Impact of nanoscale magnetite and zero valent iron on the batch-wise anaerobic Co-digestion of food waste and waste-activated sludge. *Water* 12 (5), 1283. doi:10.3390/w12051283
- Kim, H., Kim, J., Shin, S. G., Hwang, S., and Lee, C. (2016). Continuous fermentation of food waste leachate for the production of volatile fatty acids and potential as a denitrification carbon source. *Bioresour. Technol.* 207, 440–445. doi:10.1016/j.biortech.2016.02.063
- Koch, K., Plabst, M., Schmidt, A., Helmreich, B., and Drewes, J. E. (2016). Co-digestion of food waste in a municipal wastewater treatment plant: Comparison of batch tests and full-scale experiences. *Waste Manag.* 47, 28–33. doi:10.1016/j.wasman.2015.04.022
- Kucuker, M. A., Demirel, B., and Onay, T. T. (2020). Enhanced biogas production from chicken manure via enzymatic pretreatment. *J. Mat. Cycles Waste Manag.* 1, 1521–1528. doi:10.1007/s10163-020-01039-w
- Lee, C., Kim, J. Y., Lee, W. I., Nelson, K. L., Yoon, J., and Sedlak, D. L. (2008). Bactericidal effect of zero-valent iron nanoparticles on *Escherichia coli*. *Environ. Sci. Technol.* 42 (13), 4927–4933. doi:10.1021/es800408u
- Lee, Y.-J., and Lee, D.-J. (2019). Impact of adding metal nanoparticles on anaerobic digestion performance – a review. *Bioresour. Technol.* 292, 121926. doi:10.1016/j.biortech.2019.121926
- Leite, W., Magnun, B. S., Guimaraes, L. B., Gottardo, M., and Belli Filho, P. (2017). Feasibility of thermophilic anaerobic processes for treating waste activated sludge under low HRT and intermittent mixing. *J. Environ. Manag.* 201, 335–344. doi:10.1016/j.jenvman.2017.06.069
- Li, L., Hu, J., Shi, X., Fan, M., Luo, J., and Wei, X. (2016). Nanoscale zero-valent metals: A review of synthesis, characterization, and applications to environmental remediation. *Environ. Sci. Pollut. Res.* 23 (18), 17880–17900. doi:10.1007/s11356-016-6626-0
- Liao, X., Li, H., Cheng, Y., Chen, N., Li, C., and Yang, Y. (2014). Process performance of high-solids batch anaerobic digestion of sewage sludge. *Environ. Technol.* 35 (21), 2652–2659. doi:10.1080/09593330.2014.916756
- Lowry, G. V., and Reinhard, M. (2001). Pd-catalyzed TCE dechlorination in water: Effect of [H₂](aq) and H₂-utilizing competitive solutes on the TCE dechlorination rate and product distribution. *Environ. Sci. Technol.* 35 (4), 696–702. doi:10.1021/es001623f
- Métivier, H., Culleton, L., Dumont, N., Chatain, V., and Benbelkacem, H. (2020). *Handbook on characterization of Biomass, biowaste and related by-products*. 1st ed. Cham: Springer International Publishing. doi:10.1007/978-3-030-35020-8
- Mouftahi, M., Tlili, N., Hidouri, N., Bartocci, P., Alrawashdehbkoo, K. A., Gul, E., et al. (2020). Biomethanation potential (BMP) study of mesophilic anaerobic Co-digestion of abundant bio-wastes in southern regions of Tunisia. *Processes* 9 (1), 48. doi:10.3390/pr9010048
- Mu, H., Chen, Y., and Xiao, N. (2011b). Effects of metal oxide nanoparticles (TiO₂, Al₂O₃, SiO₂ and ZnO) on waste activated sludge anaerobic digestion. *Bioresour. Technol.* 102 (22), 10305–10311. doi:10.1016/j.biortech.2011.08.100
- Nduwamungu, C., Ziadi, N., Parent, L.-É., and Tremblay, G. F. (2009). Mehlich 3 extractable nutrients as determined by near-infrared reflectance spectroscopy. *Can. J. Soil Sci.* 89 (5), 579–587. doi:10.4141/cjss09018
- Oz, N. A., and Uzun, A. C. (2015). Ultrasound pretreatment for enhanced biogas production from olive mill wastewater. *Ultrason. Sonochemistry* 22, 565–572. doi:10.1016/j.ulsonch.2014.04.018
- Park, J.-H., Kang, H.-J., Park, K.-H., and Park, H.-D. (2018). Direct interspecies electron transfer via conductive materials: A perspective for anaerobic digestion applications. *Bioresour. Technol.* 254, 300–311. doi:10.1016/j.biortech.2018.01.095
- Peeters, K., Lespes, G., Zuliani, T., Ščančar, J., and Milačić, R. (2016). The fate of iron nanoparticles in environmental waters treated with nanoscale zero-valent iron, FeONPs and Fe₃O₄NPs. *Water Res.* 94, 315–327. doi:10.1016/j.watres.2016.03.004
- Peng, H., Zhang, Y., Tan, D., Zhao, Z., Zhao, H., and Quan, X. (2018b). Roles of magnetite and granular activated carbon in improvement of anaerobic sludge digestion. *Bioresour. Technol.* 249, 666–672. doi:10.1016/j.biortech.2017.10.047
- Sajid, M., Bari, S., Saif Ur Rehman, M., Ashfaq, M., Guoliang, Y., and Mustafa, G. (2022). Adsorption characteristics of paracetamol removal onto activated carbon prepared from Cannabis sativum Hemp. *Alexandria Eng. J.* 61, 7203–7212. doi:10.1016/j.aej.2021.12.060
- Sajid, M., Irfan Ahmad, M., Salman Shafiqat, S., Mulk, S., and Kamal Pasha, M. (2020). Study of Phosphorous oxide (P₂O₅) and Iron oxide (Fe₂O₃) in rock phosphate of Hazara basin of Pakistan. *Int. J. Agrochem.* 6, 1. doi:10.37628/ijac.v6i1.937
- Sekoai, P. T., Ouma, C. N. M., du Preez, S. P., Modisha, P., Engelbrecht, N., Bessarabov, D. G., et al. (2019). Application of nanoparticles in biofuels: An overview. *Fuel* 237, 380–397. doi:10.1016/j.fuel.2018.10.030
- Sounni, F., Aissam, H., Ghomari, O., Merzouki, M., and Benlemlih, M. (2017). Electrocoagulation of olive mill wastewaters to enhance biogas production. *Biotechnol. Lett.* 40 (2), 297–301. doi:10.1007/s10529-017-2464-5
- Su, L., Shi, X., Guo, G., Zhao, A., and Zhao, Y. (2013). Stabilization of sewage sludge in the presence of nanoscale zero-valent iron (nZVI): Abatement of odor and improvement of biogas production. *J. Mat. Cycles Waste Manag.* 15 (4), 461–468. doi:10.1007/s10163-013-0150-9
- Suanon, F., Sun, Q., Mama, D., Li, J., Dimon, B., and Yu, C.-P. (2016). Effect of nanoscale zero-valent iron and magnetite (Fe₃O₄) on the fate of metals during anaerobic digestion of sludge. *Water Res.* 88, 897–903. doi:10.1016/j.watres.2015.11.014
- Wu, Y., Wang, S., Liang, D., and Li, N. (2020). Conductive materials in anaerobic digestion: From mechanism to application. *Bioresour. Technol.* 298, 122403. doi:10.1016/j.biortech.2019.122403
- Xu, H., Chang, J., Wang, H., Liu, Y., Zhang, X., Liang, P., et al. (2019). Enhancing direct interspecies electron transfer in syntrophic-methanogenic associations with (semi)conductive iron oxides: Effects and mechanisms. *Sci. Total Environ.* 695, 133876. doi:10.1016/j.scitotenv.2019.133876
- Yang, Y., Guo, J., and Hu, Z. (2013). Impact of nano zero valent iron (NZVI) on methanogenic activity and population dynamics in anaerobic digestion. *Water Res.* 47 (17), 6790–6800. doi:10.1016/j.watres.2013.09.012
- Yang, Y., Zhang, C., and Hu, Z. (2013). Impact of metallic and metal oxide nanoparticles on wastewater treatment and anaerobic digestion. *Environ. Sci. Process. Impacts* 15, 39–48. doi:10.1039/c2em30655g
- Zhang, C., Su, H., Baeyens, J., and Tan, T. (2014). Reviewing the anaerobic digestion of food waste for biogas production. *Renew. Sustain. Energy Rev.* 38, 383–392. doi:10.1016/j.rser.2014.05.038
- Zhang, J., and Lu, Y. (2016). Conductive Fe₃O₄ nanoparticles accelerate syntrophic methane production from butyrate oxidation in two different lake sediments. *Front. Microbiol.* 7 (1), 1316. doi:10.3389/fmicb.2016.01316
- Zhang, Y., Yang, Z., Xu, R., Xiang, Y., Jia, M., Hu, J., et al. (2019). Enhanced mesophilic anaerobic digestion of waste sludge with the iron nanoparticles addition and kinetic analysis. *Sci. Total Environ.* 683, 124–133. doi:10.1016/j.scitotenv.2019.05.214
- Zhao, Z., Li, Y., Yu, Q., and Zhang, Y. (2018). Ferroferric oxide triggered possible direct interspecies electron transfer between *Syntrophomonas* and *Methanosaeta* to enhance waste activated sludge anaerobic digestion. *Bioresour. Technol.* 250, 79–85. doi:10.1016/j.biortech.2017.11.003